Available online at www.sciencedirect.com

ScienceDirect

IFAC Papers Online CONFERENCE PAPER ARCHIVE

IFAC-PapersOnLine 48-8 (2015) 1120–1125

Integrated Process Design and Control of Reactive Distillation Processes

Seyed Soheil Mansouri[a], Mauricio Sales-Cruz[b], Jakob Kjøbsted Huusom[a], John M. Woodley[a], Rafiqul Gani[a,*]

[a]*CAPEC-PROCESS, Department of Chemical and Biochemical Engineering, Technical University of Denmark, Lyngby, Denmark*

[b]*Departamento de Procesos y Tecnología, Universidad Autónoma Metropolitana-Cuajimalpa, México D.F., Mexico*

(*e-mails: seso@kt.dtu.dk, asales@correo.cua.uam.mx, jkh@kt.dtu.dk, jw@kt.dtu.dk, rag@kt.dtu.dk*)

Abstract: In this work, integrated process design and control of reactive distillation processes is presented. Simple graphical design methods that are similar in concept to non-reactive distillation processes are used, such as reactive McCabe-Thiele method and driving force approach. The methods are based on the element concept, which is used to translate a system of compounds into elements. The operation of the reactive distillation column at the highest driving force and other candidate points is analyzed through analytical solution as well as rigorous open-loop and closed-loop simulations. By application of this approach, it is shown that designing the reactive distillation process at the maximum driving force results in an optimal design in terms of controllability and operability. It is verified that the reactive distillation design option is less sensitive to the disturbances in the feed at the highest driving force and has the inherent ability to reject disturbances.

Keywords: Process design, Process control, Driving force , Reactive distillation, Element-based method

1. INTRODUCTION

Traditionally, process design and process control are considered as independent problems, that is, a sequential approach is used where the process is designed first, followed by the control design. The limitations with the sequential approach are related to dynamic constraint violations, for example, infeasible operating points, process overdesign or under-performance. Therefore, this approach does not guarantee robust performance (Seferlis and Georgiadis, 2004). Furthermore, process design decisions can influence process control and operation. To overcome the limitations associated with the sequential approach, operability and controllability are considered simultaneously with process design, in order to assure that design decisions give the optimum operational and economic performance. In control design, operability addresses stability and reliability of the process using *a priori* operational conditions and controllability addresses maintaining desired operating points of the process subject to disturbances.

A number of methodologies and tools have been proposed and applied on various problems to address the interactions between process design and control, and they range from optimization-based approaches to model-based methods (Luyben and Floudas, 1994; Nikacevic *et al.*, 2012).

In this work, integrated design and control of reactive distillation processes is considered, since process design decisions will influence process operability and controllability. Numerous design algorithms for multi-component separation systems with reactions have accompanied the increasing interest in reactive distillation processes. In design, the input and (selected) output variables are specified and the task is to determine the optimal reactive distillation process configuration (for example, minimum number of stages), and the optimal design parameters (for example, optimum reflux ratio, optimal feed location) that achieve the given product specification. It is intended to achieve the optimal design in such way that it is also an operable process at pre-defined conditions under presence of disturbances.

P□rez-Cisneros *et al.* (1997) have proposed an element mass balance approach to design the reactive distillation processes, which employs the traditional graphical tools similar in concept to design of non-reactive distillation columns, such as McCabe-Thiele method and driving force approach of Bek-Pedersen and Gani (2004). Moreover, Hamid *et al.* (2010) have proposed an integrated process design and controller design methodology. However, their methodology covers the aspects related to design and control of non-reactive binary distillation processes. In this work, the method of Hamid *et al.* (2010) is extended to also cover a ternary compound reactive distillation process (using element-based approach) and criteria of selecting the optimal design and the controller structure selection will be presented. In order to demonstrate the application of the aforementioned approach, production of methyl-tert-butyl-ether (MTBE)

* Corresponding Author: rag@kt.dtu.dk (Rafiqul Gani)

10.1016/j.ifacol.2015.09.118

from methanol and isobutene using a reactive distillation column is considered.

2. REACTIVE DISTILLATION COLUMN DESIGN

The computation of simultaneous chemical and physical equilibrium plays an important role in the prediction of the limits for conversion and separation of a specific reactive separation process, particularly for the reactive distillation systems. Using the Gibbs free energy minimisation approach, P□rez-Cisneros *et al.* (1997) proposed solution procedures where the multicomponent chemical and physical equilibrium is posed as an "element phase" equilibrium problem. This transformation is based on the concept of chemical model as proposed by Michelsen (1989). This concept is derived from chemical model theory. In chemical model theory, the equations of chemical equilibrium and any appropriate physical model yielding the chemical potentials are incorporated into an element-based model (called the chemical model). The chemical model algorithm and those developed earlier, differ in the use of the chemical models in a way that reduces the chemical and physical equilibrium problem formally identical to the physical equilibrium problem for a mixture of elements (representing the system). Further details can be found in (P□rez-Cisneros, 1997; Daza *et al.*, 2003). The reaction for MTBE synthesis occurs very fast, therefore, chemical equilibrium is assumed (for other cases a kinetic model may be used) and is given as follows:

$$Isobutene\left(C_4H_8\right)+Methanol\left(CH_4O\right)\rightleftarrows MTBE\left(C_5H_{12}O\right)$$

It is clear that the selection of the elements has an important role in the current formulation. They are normally chosen as the "natural" chemical elements present in the reaction mixture. However, one is free to select any reaction invariant fragment of the reactants. The element matrix is constructed based on the rules provided by P□rez-Cisneros *et al.* (1997) and it is as follows:

	Component		
Element	**C_4H_8 (1)**	**CH_4O (2)**	**$C_5H_{12}O$ (3)**
A	1	0	1
B	0	1	1

Therefore, the ternary system of compounds can be reduced into a binary system of elements *A* and *B* and the reaction can be rewritten as: $A+B\rightleftarrows AB$. The first component (element *A*) and the second component (element *B*) form the third component (element *AB*). Having the ternary system of compounds represented in form of a binary element system, similar graphical design methods, that are applied to non-reactive binary distillation column design, such as McCabe-Thiele method can be used. However, in order to use the McCabe-Thiele method, a reactive equilibrium curve is required. The reactive equilibrium curve is constructed through sequential computation of reactive bubble points (P□rez-Cisneros, 1997). In order to generate the reactive data-set, Wilson thermodynamic model for prediction of the liquid phase behaviour and SRK equation of state for prediction of vapour phase behaviour were used. Note that the calculation of reactive vapour-liquid equilibrium (VLE) data set is in terms of compounds. Therefore, a ternary compound data set is obtained. To convert this data set to be represented in form of a binary element system the following expressions are used where mole fractions of elements *A* and *B* are calculated in the liquid phase:

$$W_A^l=\frac{x_1+x_3}{x_1+x_2+2\cdot x_3} \tag{1}$$

$$W_B^l=\frac{x_2+x_3}{x_1+x_2+2\cdot x_3} \tag{2}$$

In the above equations W_A^l and W_B^l are the liquid mole fractions of elements *A* and *B*, respectively. For calculation of the element mole fractions in vapour phase (W_A^v and W_B^v), the equations used are the same as (1) and (2) where instead of liquid molar fraction (x_i), the vapour molar fraction (y_i) is used. Fig. 1 depicts the temperature (*T*)-W_A diagram for MTBE reactive system. Note that as long as $NC - R = 2$ (*NC* is number of compunds and *R* is number of reactions), any system can be representd by two elements (P□rez-Cisneros et al., 1997).

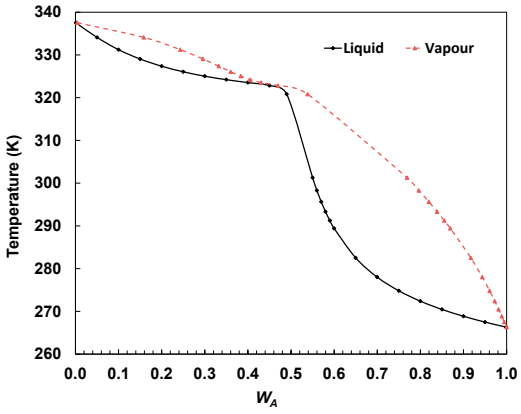

Fig. 1. *T*-W_A^v-W_A^l diagram for MTBE reactive system (*P* = 1 atm).

The design task is to separate a binary element mixture that is 70 mole percent element *A* (z_{WAf} = $z_{isobutene}$ = 0.7, z_{WBf} = $z_{methanol}$ = 0.3) into 50 element mole percent bottoms product ($W^l_{A,B}$ = 0.50) and 99 element mole percent distillate ($W^l_{A,d}$ = 0.99) product. Note that based on the binary element reaction matrix, element *A* and *B* correspond to isobutene and methanol, respectively. The element feed flow rate is 100 Kg-mole element/hr at 300K and 1 atm. The operating pressure of the reactive distillation column is 1 atm and pressure drop across the column is assumed to be negligible. The reflux element ratio (RR) is 2. The physical and chemical equilibrium curve is constructed using the data set presented in Fig. 1. Theoretical reactive stages are calculated from the reactive McCabe-Thiele method. A partial reboiler, total condenser and chemically saturated liquid reflux are set for the column. In order to design the described reactive distillation column for MTBE synthesis, McCabe-Thiele method is used. Fig. 2 depicts the reactive distillation column design using reactive McCabe-Thiele method. As it is shown in Fig. 2, the reactive distillation column has five reactive stages.

Daza *et al.* (2003) have extended the driving force (DF_i) method for non-reactive systems (Bek-Pedersen and Gani, 2004) to include reactive systems. Similar in concept to non-reactive systems, the driving force is defined as the difference in composition between two coexisting phases. The driving-force design method for reactive as well as non-reactive distillation systems is based on the availability of data for the vapour-liquid behaviour. In the case of reactive systems, the vapour-liquid equilibrium data must be based on the elements (see Fig. 1).

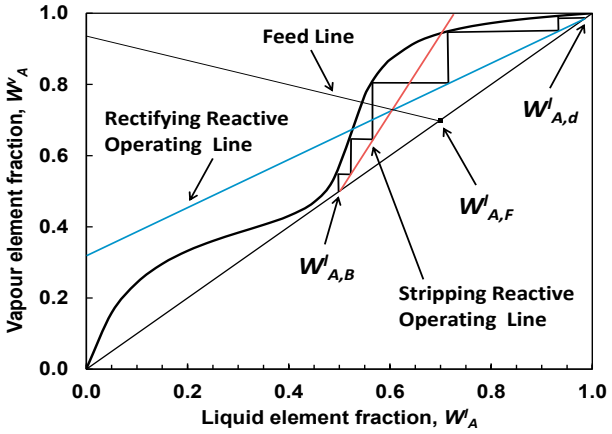

Fig. 2. Reactive distillation column design using reactive McCabe-Thiele method for the MTBE reactive system.

The driving-force diagram can only represent binary interaction between compounds or elements in two co-existing phases, or two compounds on a solvent-free basis. Note that the element-based driving-force diagram fully considers the extent of reaction on an element basis, and it can be applied in the design of reactive distillation columns. Provided the element vapour-liquid behaviour data exist (equilibrium or rate-based), or can be computed (which is the case in this study, see Fig. 1), the reactive driving-force diagram can be obtained using (3) with respect to elements.

$$DF_i = W_i^v - W_i^l = \frac{W_i^l \alpha_{ij}}{1 + W_i^l \left(\alpha_{ij} - 1\right)} - W_i^l \qquad (3)$$

Note that in (3), The relative separability α_{ij} is a parameter for component i with respect to property (or separation technique) j (Bek-Pedersen and Gani (2004). The driving force concept is used to find the optimal design target values of the process variables for separation systems. Based on identification of the largest driving force (see Fig. 3), defined as the difference in composition of a component i between the vapour phase and the liquid phase, which is caused by the difference in the volatilities of component i and all other components in the system. Fig. 3 shows the driving force diagram for MTBE reactive system at 1 atm. As the driving force decreases, separation becomes difficult and may become infeasible when the driving force approaches zero. On the other hand, as the driving force approaches its maximum value, the separation becomes easier. Therefore, from a process design point of view, a separation process should be designed/selected at the highest possible driving force, which will naturally lead to the optimal design with respect to the energy consumption (Bek-Pedersen and Gani (2004)).

In this work, the optimal feed location of the reactive distillation column is determined using the driving force diagram. Reactive McCabe-Thiele method has been only used to determine the number of stages. The feed and product specifications are already known since they were used in the reactive McCabe-Thiele method. The optimal feed location at the maximum driving force can be found using (4).

$$N_F = N\left(1 - D_x\right) \qquad (4)$$

In (4), N is the number of stages which was obtained from the reactive McCabe-Thiele method (was found to be 5); D_x is the value corresponding to the maximum driving force on the x-axis (D_x = 0.61). The optimal feed location is identified using the additional rules for driving force (Bek-Pedersen and Gani, 2004) and therefore it is stage 1 from the top of the column.

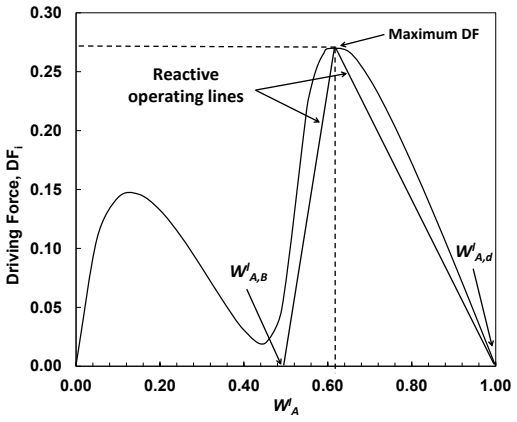

Fig. 3. Reactive driving force diagram for MTBE reactive system.

3. OPTIMAL DESIGN-CONTROL SOLUTIONS

From a process design point of view, for specified inputs, u, and disturbances, d, values for states, x, and outputs, y, that satisfy a set of design specifications (process design objectives) are determined. In this case, x and y also define some of the operational conditions for the process. From a controller design point of view, for any changes in d and/or set point values in y, values of u that restores the process to its optimal designed condition are determined. It should be noted that the solution for x and y is directly influenced by θ (the constitutive variables such as reaction rate or equilibrium constant). For example, the optimal solution for x and y can be obtained at the maximum point of the reactive driving force (for reactive systems, see Fig. 3) diagrams which are based on θ. By using model analysis, the corresponding derivative information with respect to x, y, u, d and θ can be obtained (to satisfy controller design objectives).

For each reactive distillation column design problem, the driving force diagram is drawn and the design target is selected at the highest driving force (see Fig. 3). From a process design point of view, at these targets, the optimal design objectives can be obtained. From a controller design point of view, at these design targets the controllability and

operability of the process is best satisfied. The value of the derivative of controlled variables y with respect to disturbances in the feed, d, dy/dd and manipulated variables, u, dy/du will determine the process sensitivity and influence the controller structure selection. Accordingly, dy/dd and dy/du are defined as (Russel et al., 2002):

$$\frac{dy}{dd}=\left(\frac{dy}{d\theta}\right)\left(\frac{d\theta}{dx}\right)\left(\frac{dx}{dd}\right) \tag{5}$$

$$\frac{dy}{du}=\left(\frac{dy}{d\theta}\right)\left(\frac{d\theta}{dx}\right)\left(\frac{dx}{du}\right) \tag{6}$$

The values for dθ/dx can be obtained from the process (dynamic and/or steady state) constraints:

$$\frac{dx}{dt}=f\left(x,y,u,d,\theta,Y,t\right) \tag{7}$$

and values for dy/dθ, dx/dd and dx/du can be obtained from constitutive (thermodynamic) constraints:

$$0=g\left(u,x,y\right)-\theta \tag{8}$$

3.1. Selection of Controlled Variables

The primary controlled variable is $D_{x,max}$, which is the x-axis value corresponding to the maximum driving force (DF$_i$). This resembles the purity of element A at the maximum driving force. The secondary controlled variables are the product purities, which are the desired product composition at the top and bottom of the column, $W_A^{\,d}$ and $W_A^{\,B}$. The reason behind this selection is that by controlling $W_A^{\,d}$ and $W_A^{\,B}$ at the maximum point of the driving force will require less control effort in terms of reflux ratio (RR), and reboil ratio (RB) in the presence of disturbances in the feed compared to any other candidate point.

3.2. Sensitivity of Controlled Variables to Disturbances

Using the below key concepts, the sensitivity of variable y with respect to variable d can be expressed as in (9):

- The desired element product at the top and the bottom is $W_A^{\,d}$ (product element composition at the top, distillate product) and $W_A^{\,B}$ (element composition at the bottom, bottom product).
- At the maximum point of the driving force diagram, $W_A^{\,d}$ and $W_A^{\,B}$ (controlled variables) are the least sensitive to the imposed disturbances in the feed.
- The design variables vector is $y = [W_A^{\,d} \quad W_A^{\,B}]$, x = DF$_i$, is selected on the y-axis of the driving force diagram.
- The disturbances vector is, d = [F$_f$ z_{WAf}] (feed flowrate and feed composition of element A).

$$\frac{dy}{dd}=\begin{bmatrix}\frac{dW_A^d}{dF_f} & \frac{dW_A^d}{dz_{W_{Af}}}\\ \frac{dW_A^B}{dF_f} & \frac{dW_A^B}{dz_{W_{Af}}}\end{bmatrix}= \begin{bmatrix}\left(\frac{dW_A^d}{dDF_i}\right)\left(\frac{dDF_i}{dW_A^l}\right)\left(\frac{dW_A^l}{dF_f}\right) & \left(\frac{dW_A^d}{dDF_i}\right)\left(\frac{dDF_i}{dW_A^l}\right)\left(\frac{dW_A^l}{dz_{W_{Af}}}\right)\\ \left(\frac{dW_A^B}{dDF_i}\right)\left(\frac{dDF_i}{dW_A^l}\right)\left(\frac{dW_A^l}{dF_f}\right) & \left(\frac{dW_A^B}{dDF_i}\right)\left(\frac{dDF_i}{dW_A^l}\right)\left(\frac{dW_A^l}{dz_{W_{Af}}}\right)\end{bmatrix} \tag{9}$$

The reactive element operating lines for the rectifying section and stripping sections are given in (10) and (11). RR is the element reflux ratio, and RB is the element reboil ratio.

$$W_A^v=\frac{RR}{RR+1}W_A^l+\frac{1}{RR+1}W_A^d \tag{10}$$

$$W_A^v=\frac{RB+1}{RB}W_A^l-\frac{1}{RB}W_A^B \tag{11}$$

Substituting (10) and (11) in (3) for $W^v{}_A$ gives the top and bottom element product composition with respect to the driving force in (12) and (13) which is:

$$W_A^d=DF_i\left(RR+1\right)+W_A^l \tag{12}$$

$$W_A^B=W_A^l-DF_iRB \tag{13}$$

Equations (12) and (13) are differentiated with respect to DF$_i$ and result in the following expressions:

$$\frac{dW_A^d}{dDF_i}=\left(RR+1\right)+\frac{dW_A^l}{dDF_i}=\left(RR+1\right)+\left(\frac{dDF_i}{dW_A^l}\right)^{-1} \tag{14}$$

$$\frac{dW_A^B}{dF_{Di}}=\frac{W_A^l}{dDF_i}-RB=\left(\frac{dDF_i}{dW_A^l}\right)^{-1}-RB \tag{15}$$

The total element A mass balance is written as follows:

$$F_f\cdot z_{W_{Af}}=W_A^db^d+W_A^Bb^B \tag{16}$$

Where, b^d and b^B are element A mass flows in top and bottom of the column, respectively. Substituting (12) and (13), one at the time, into (16) for $W_A^{\,d}$ and $W_A^{\,B}$, the total element A mass balance in terms of driving force is expressed as:

$$F_f\cdot z_{W_{Af}}=DF_i\left(RR+1\right)b^d+W_A^lb^d+W_A^Bb^B \tag{17}$$

or

$$F_f\cdot z_{W_{Af}}=W_A^db^d+W_A^lb^B-b^BF_{Di}RB \tag{18}$$

Differentiating (17) and (18) with respect to the F_f and z_{WAf} (assuming that the changes in composition, and, top and bottom element flowrates (b^d and b^B) with respect to the feed flowrate is negligible), the expressions for dW_A^l/dF_f, $dW_A^l/dz_{W_{Af}}$ are obtained. Having these derivatives, the solution to (9) is expressed by (19). Note that in (19), a_1,.., a_8 are constants.

Values of dFD$_i$/d$W_A^{\,l}$ are calculated and shown in Fig. 4. Note that in Fig. 4, two other points (points II and III) which are not at the maximum are identified as candidate alternative designs for a distillation column, which will be used for verification purposes. Note that operation at the maximum driving force does not restrict achievable design performance (for example, component purities).

It must be noted that the expressions for $\left(dW_A^d/dDF_i\right)\left(dDF_i/dW_A^l\right)$ and $\left(dW_A^B/dDF_i\right)\left(dDF_i/dW_A^l\right)$ in

(19) are equal to 1 at point (I) in Fig. 4 (maximum driving force) and greater than 1 in any other point.

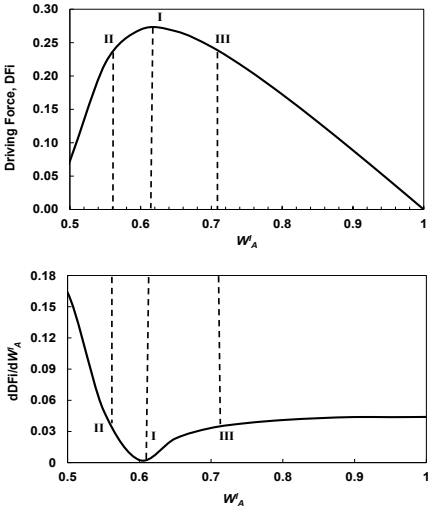

Fig. 4. Driving force diagram for W_A–W_B separation (reactive zone only – top figure) and its corresponding derivative of FDi with respect to W_A^l (bottom figure).

$$\begin{bmatrix} \frac{dW_A^d}{dF_f} \\ \frac{dW_A^B}{dF_f} \\ \frac{dW_A^d}{dz_{W_{Af}}} \\ \frac{dW_A^B}{dz_{W_{Af}}} \end{bmatrix} = \begin{bmatrix} \left((RR+1)+\left(\frac{dDF_i}{W_{Ai}^l}\right)^{-1}\right)\left(\frac{dDF_i}{dW_{Ai}^l}\right)\left(\frac{a_1}{\left[a_2\frac{dDF_i}{dW_A^l}+a_3+\left(\frac{dW_A^d}{dDF_i}\right)\left(\frac{dDF_i}{dW_A^l}\right)\right]}\right) \\ \left(\left(\frac{dDF_i}{dW_A^l}\right)^{-1}-RB\right)\left(\frac{dDF_i}{dW_{Ai}^l}\right)\left(\frac{a_4}{\left[a_5\frac{dDF_i}{dW_{Ai}^l}+a_6+\left(\frac{dW_A^B}{dDF_i}\right)\left(\frac{dDF_i}{dW_{Ai}^l}\right)\right]}\right) \\ \left((RR+1)+\left(\frac{dDF_i}{W_{Ai}^l}\right)^{-1}\right)\left(\frac{dDF_i}{dW_{Ai}^l}\right)\left(\frac{a_7}{\left[a_2\frac{dDF_i}{dW_A^l}+a_3+\left(\frac{dW_A^d}{dDF_i}\right)\left(\frac{dDF_i}{dW_A^l}\right)\right]}\right) \\ \left(\left(\frac{dDF_i}{dW_A^l}\right)^{-1}-RB\right)\left(\frac{dDF_i}{dW_{Ai}^l}\right)\left(\frac{a_8}{\left[a_5\frac{dDF_i}{dW_{Ai}^l}+a_6+\left(\frac{dW_A^B}{dDF_i}\right)\left(\frac{dDF_i}{dW_{Ai}^l}\right)\right]}\right) \end{bmatrix} \quad (19)$$

Furthermore, at point A the value of $\mathrm{dFD}_i/\mathrm{d}W_A^l$ is equal to zero. Therefore, equation (19) at Point A (maximum driving force) can be expressed as:

$$\frac{dy}{dd} = \begin{bmatrix} \frac{dW_A^d}{dF_f} & \frac{dW_A^B}{dF_f} \\ \frac{dW_A^d}{dz_{W_{Af}}} & \frac{dW_A^B}{dz_{W_{Af}}} \end{bmatrix} \approx \begin{bmatrix} (0)\left(\frac{a_1}{a_3+1}\right) & (0)\left(\frac{a_4}{a_6+1}\right) \\ (0)\left(\frac{a_7}{a_3+1}\right) & (0)\left(\frac{a_8}{a_6+1}\right) \end{bmatrix} \approx \begin{bmatrix} 0 & 0 \\ 0 & 0 \end{bmatrix} \quad (20)$$

Equation (20) reveals that the sensitivity of controlled variables to disturbances in the feed is minimum at the maximum driving force.

3.3. Selection of the Controller Structure

The controlled variables are defined as top and bottom element A composition W_A^d and W_A^B. In this case, the potential manipulated variables are reflux ratio (RR) and reboil ratio (RB). (12) and (13) give the top and bottom product compositions with respect to the driving force. Hence, they are differentiated with respect to *RR* and *RB*. Therefore, (6) can now be expressed as:

$$\frac{dy}{du} = \begin{bmatrix} \frac{dW_A^d}{dRR} & \frac{dW_A^d}{dRB} \\ \frac{dW_A^B}{dRR} & \frac{dW_A^B}{dRB} \end{bmatrix} = \begin{bmatrix} DF_i+(RR+1)\left(\frac{dDF_i}{dW_{Ai}^l}\right)\left(\frac{dW_A^l}{dRR}\right)+\frac{dW_A^l}{dRR} & (RR+1)\left(\frac{dDF_D}{dW_A^l}\right)\left(\frac{dW_A^l}{dRB}\right)+\frac{dW_A^l}{dRB} \\ \frac{dW_A^l}{dRR}-\left(\frac{dDF_i}{dW_A^l}\right)\left(\frac{dW_A^l}{dRR}\right)RB & \frac{dW_A^l}{dRB}-DF_i \end{bmatrix} \quad (21)$$

From Fig. 4, it is known that dDF_i/dW_A^l at the maximum driving force is equal to zero. Furthermore, assuming that $dW_A^l/dRR = dW_A^l/dRB = 0$, (22) is obtained. The best controller structure can easily be determined by looking at the value of d*y*/d*u*. It can be noted from (22) that since the values of dW_A^d/dRR and dW_A^B/dRB are bigger, controlling W_A^d by manipulating *RR* and controlling W_A^B by manipulating *RB* will require less control action.

$$\frac{dy}{du} = \begin{bmatrix} \frac{dW_A^d}{dRR} & \frac{dW_A^d}{dRB} \\ \frac{dW_A^B}{dRR} & \frac{dW_A^B}{dRB} \end{bmatrix} = \begin{bmatrix} DF_i & 0 \\ 0 & -DF_i \end{bmatrix} \quad (22)$$

This is because only small changes in *RR* and *RB* are required to move W_A^d and W_A^B in a bigger direction. This pairing between controlled-manipulated variables is also further verified by obtaining the transfer functions between the pairs using a reactive distillation dynamic model based on elements (Pérez-Cisneros, 1997). Note that most of the modelling of dynamic reactive distillation operations has been done by introducing a rate of reaction expression in the component mass balances. However, when the chemical reactions occurring are fast enough to reach the equilibrium (for MTBE reactive system) chemical equilibrium condition is implicitly incorporated into the element mass balances through the functionality of the phase compositions on the element chemical potentials (Pérez-Cisneros, 1997).

The next natural step to verify the pairing in (22) is calculating the relative gain array (RGA) for the design at the optimal feed location (Design (I), N_F = 1) and two other alternative designs (Design (II), N_F = 2; and Design (III), N_F = 3). Note that in calculating RGA, *RB* is represented by heat addition to the reboiler duty instead of reboil ratio; and, MTBE top and bottom compositions represent W_A^d and W_A^B, respectively. The transfer functions have the form as equation (23) with one zero and two poles.

$$G(s) = K\frac{1+\tau_z s}{(1+\tau_{p1}s)(1+\tau_{p1}s)} \quad (23)$$

Using the transfer functions, RGA matrix for design (I) (at the maximum driving force) and designs (II) and (III) is calculated and they are as follows:

$$RGA_{(I)} = \begin{bmatrix} 0.93 & 0.07 \\ 0.07 & 0.93 \end{bmatrix}, RGA_{(II)} = \begin{bmatrix} 9.06 & -8.06 \\ -8.06 & 9.06 \end{bmatrix}, RGA_{(III)} = \begin{bmatrix} -0.28 & 1.28 \\ 1.28 & -0.28 \end{bmatrix}$$

As it can be seen the pairing at the maximum driving force (design (I), feed location 1) has the closest values on the diagonal to unity. Therefore, it has the least interaction between the loops. Furthermore, the suggested pairing by RGA for design (I) matches the pairing that was obtained from the driving force. Furthermore, singular value analysis

(SVA) was performed. However, very large condition numbers (CN) were obtained with no specific trend. Thus, no particular conclusion can be made based on them. The open-loop and closed-loop performance of the system has been tested with the Proportional-Integral (PI) controller in a discrete-time manner. The rigours dynamic reactive distillation model (P□rez-Cisneros, 1997) was used. The controller implementation is visualized in Fig. 5. Note, however, any other control strategy can be applied to perform closed-loop simulations.

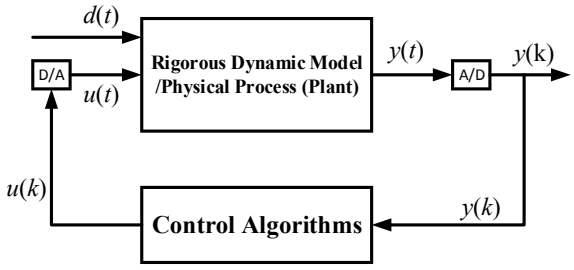

Fig. 5. Discrete-time controller structure implementation.

Fig. 6 and Fig. 7 show the open-loop and closed-loop performance of the system at maximum driving force (Design (I)), respectively. The disturbance scenario is that after 15 samples, the feed flowrate of element A (isobutene) is increased from 70 kg-mole to 85 kg-mole (~12% step change in composition of isobutene).

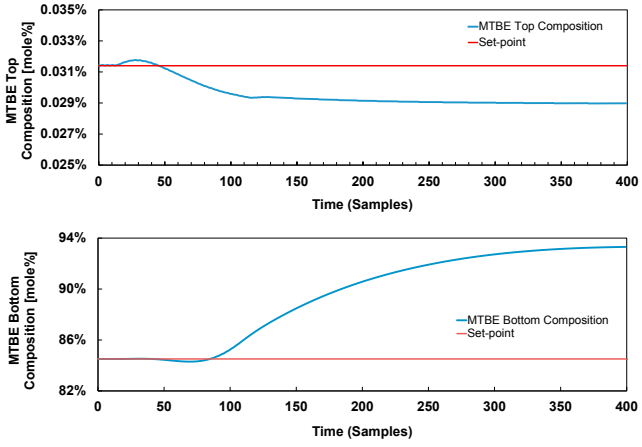

Fig. 6. Open-loop performance of Design (I) to a disturbance in the feed.

This disturbance results in a change in total feed flowrate by +15% and also a change in the feed composition. As it can be seen in Fig. 6, as a result of an increased isobutene flowrate, its recovery in the top has increased which results in a lower MTBE composition in the top. Furthermore, because of excess isobutene in the system and thereby shifting the reaction equilibrium, MTBE composition has increased in the bottom. It can be seen in Fig. 7 that disturbance has been rejected with least interaction between the loops and both top and bottom compositions are well controlled using the selected pairing obtained from the driving force. Note that the control of the MTBE top composition is achieved with very small changes in *RR*.

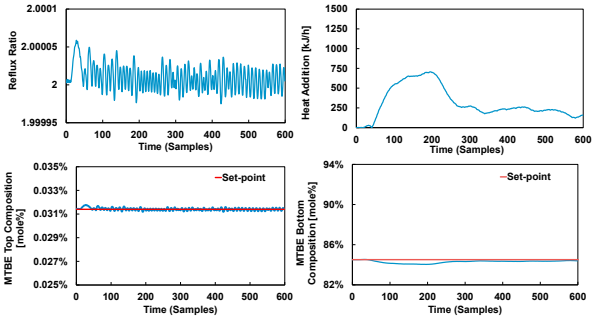

Fig. 7. Closed-loop performance of the control structure for Design (I) to a disturbance in the feed.

4. CONCLUSIONS

Integrated process design and control of a ternary compound reactive distillation process was investigated in this work. The optimal design-control solutions were obtained analytically and verified through rigorous dynamic simulations. It is verified that the reactive distillation design option is less sensitive to the disturbances in the feed at the highest driving force and has the inherent ability to reject disturbances. Furthermore, it is advantageous to employ the element-based method for designing multi-component and complex reacting systems.

REFERENCES

Bek-Pedersen, E., Gani, R. (2004). Design and synthesis of distillation systems using a driving-force-based approach, *Chem. Eng. Process.*, 43, 251–262

Daza, O.S., P□rez-Cisneros, E.S., Gani, R. (2003). Graphical and stage-to-stage methods for reactive distillation column design, *AIChE J.*, 49, 2822-2841.

Hamid, M. K. A., Sin, G., and Gani, R. (2010). Integration of process design and controller design for chemical processes using model-based methodology. *Comput. Chem. Eng.*, 34, 683-699.

Luyben, M. L., Floudas, C. A. (1994). Analyzing the interaction of design and control – 2. Reactor-Separator-Recycle system, *Comput. Chem. Eng.*, 18, 971-994.

Michelsen, M.L. (1989). Calculation of Multiphase Ideal Solution Chemical Equilibrium, *Fluid Phase Equilib.*, 53, 73-80.

Nikacevica, N.M., Huesman, A.E.M., Van den Hof, P.M.J., Stankiewicz, A.I. (2012). Opportunities and challenges for process control in process intensification, *Chem. Eng. Process.*, 52, 1-15.

P□rez-Cisneros, E.S., Gani, R., Michelsen, M.L. (1997). Reactive separation systems—I. Computation of physical and chemical equilibrium, *Chem. Eng. Sci.*, 52, 527–543.

P□rez-Cisneros, E.S. (1997). *Modelling, design and analysis of reactive separation processes*, Ph.D. Thesis, Technical University of Denmark, Lyngby.

Russel, B. M., Henriksen, J. P., J□rgensen, S. B., Gani, R. (2002). Integration of design and control through model analysis. *Comput. Chem. Eng.*, 26, 213-225.

Seferlis, P., Georgiadis, M. C. (2004). *The integration of process design and control*, Elsevier B. V., Amsterdam.